Hariram et al. 2018. *Int. J. Vehicle Structures & Systems*, 10(6), 423-432
ISSN: 0975-3060 (Print), 0975-3540 (Online)
doi: 10.4273/ijvss.10.6.11

International Journal of Vehicle Structures & Systems
Available online at www.maftree.org/eja

Effect of Carbon Nanotubes on Oxygenated Jojoba Biodiesel-Diesel Blends in Direct Injection CI Engines

V. Hariram[a], V. Udhayakumar, P. Karthick, A. Abraham Eben Andrews, A. Arunraja, S. Seralathan and T. Micha Premkumar

Dept. of Mech. Engg., Hindustan Institute of Tech. and Sci., Chennai, India
[a]Corresponding Author, Email: connect2hariram@gmail.com

ABSTRACT:

Scarcity and inflated cost of petroleum reserves along with environmental pollution concerns urged the researchers to identify a better alternative source of eco-friendly bio-energy. In this study, oxygenated biodiesel derived from Jojoba oil was used in a compression ignition engine to analyse the engine characteristics in the presence of multi-walled carbon Nanotubes (MWCNT) at 50 ppm, 100 ppm and 150 ppm concentrations. Taguchi's approach based experimentation identified the stability of modified fuel blends ratios of n-butanol, biodiesel and MWCNT. The Jojoba biodiesel was characterized using FTIR and GC MS techniques to understand the presence of fatty acid methyl esters in the biodiesel. Higher brake thermal efficiency and significant reduction in specific fuel consumption were observed in fuel blend with MWCNT. D70JJBD20O10CNT100 showed higher in-cylinder pressure and heat release rate due to micro-explosion of carbon nanotubes at full load condition. The ignition delay was also significantly affected with the addition of MWCNT. The exhaust emission like un-burned hydrocarbon, oxides of carbon, oxides of nitrogen and smoke exhibited noticeable variations with the modified fuel blends.

KEYWORDS:

Biodiesel; Multi-walled carbon nano tubes; n-butanol; Performance; Combustion; Emission

CITATION:

V. Hariram, V. Udhayakumar, P. Karthick, A.A.E. Andrews, A. Arunraja, S. Seralathan and T.M. Premkumar. 2018. Effect of Carbon Nanotubes on Oxygenated Jojoba Biodiesel-Diesel Blends in Direct Injection CI Engines, *Int. J. Vehicle Structures & Systems*, 10(6), 423-432. doi:10.4273/ijvss.10.6.11.

1. Introduction

There is an increase in the demand for fossil fuel in and around our country, and to meet the demand for future generation, researchers are experimenting on energy conservation methods like alternative fuels, fuel cells, and hybrid fuel. For past three decades, scientists have been improvising the alternative fuel by adding oxygenated compounds and nano-additives to the fuel. The usage of oxygenated compounds in the fuel tends to improve the parameters like combustion behaviour, performance and emission. Moreover, using of nano-particles has created a great scope in the alternative fuel. Numerous researches have been conducted in alternative fuel with different oils (pongamia, rape-seed, jatropha, jojoba, lemon grass, waste cooking oil etc.). Even though there is a lot of improvement in the engine dimensions for a better fuel economy, these kinds of efforts is not that much satisfactory to overcome an optimized result. Therefore, fuel improvisation would be preferable to meet the better combustion and performance without compromising the emission norms [1-4].

There are significant engine parameters like compression ratio, exhaust gas temperature, injection pressure, injection timing that are taken into consideration while implementing the biodiesel by adding alcoholic groups like n-butanol, di-ethyl ether, ethanol and methanol. From a variety of parameters, injection pressure and injection timing can be combined to make strategies in methanol blended fuel and eventually reducing the un-burnt hydrocarbon (UBHC) and carbon monoxide (CO) but with a higher nitrogen oxide (NO_x). Even injection strategies play a key role in diminishing the exhaust emission in a highly considerable manner [5-7]. Generally, there is a threat to all human kind because of the climate change and global warming issues. Dominantly, there are two medium of transport facilities available: (a) diesel powered automotive transportation and (b) gasoline powered automotive transportation. Diesel powered transportation gives 25-35% better mileage and emits less CO_2 than gasoline-powered transportation.

For the above reasons and to sustain an ecological balance, a lot of research was directed on alternative fuels. At the same time, considering the massive population growth around the world, researchers prefer non-edible oils to do the experimentation on alternate fuels. Using non-edible oil will meet the demands of the forthcoming generation. There are many non-edible oils available in the global market, namely karanja, jatropha, jojoba, rapeseed, animal fat, pongamia and canola, etc. Adding alcohols in the biodiesel improves the volatility and latent heat property. Though researchers use alcoholic content, the disadvantage like layer separation, agglomeration might take place. While experimenting with biodiesel and alcohols, there are numerous options

available for the researchers. Alcoholic content like ethanol, methanol, diethyl ether, n-butanol, dimethyl ether are dominantly practiced by the scientists. For the past few decades, researchers have given promising results by reducing the CO and NO_x emissions by adding alcoholic content in the biodiesel [8, 9]. Therefore, for a good combustion, there is a need for enough of oxygen (in form of oxygenated compounds or alcoholic content) to be given in the combustion chamber.

By reviewing the earlier researches, it is found that the researchers focused on increasing the performance characteristics like brake thermal efficiency (BTE), reducing the brake specific fuel consumption (BSFC) and emission from the exhaust and ensuring that no knocking or detonation tends to happen while experimenting with alternative fuels. Choudhury et al [10] experimented on the mechanical stirring and sonication for the acid catalyzed esterification of jatropha oil. The acid catalyze was not very much reactive to ultrasound sonication. The author concluded that the sonication process did not change the chemistry of the process and the beneficial effect on the physical nature was further limited by intrinsic kinetics and mass transfer. Paul et al [11] investigated jatropha biodiesel for engine test and concluded that there was a declension in torque and BTE. As the blend proportion became more, simultaneously there was a decrease in the torque and BTE and BSFC increased with more amount of jatropha biodiesel in the blend. There was an increase in the NO_x compared to base diesel due to higher oxygen content in the jatropha oil. However, there was a complete combustion and there was also a rise in temperature of the combustion chamber.

Raheman et al [12] concluded that blended fuel emulsified jatropha blends showed pressure crank angle like diesel and no unsuitable combustion features like unacceptable high cylinder gas pressure. BTE with emulsified biodiesel blend at low and high load was estimated to be 1-2% lower than biodiesel blend and 3-4% respectively because of micro explosion. Emissions like carbon dioxide was 7-8% lower, HC 31.5- 51.5% lesser than that of JB10 and base diesel. At lower and higher loads, CO emissions were reduced by 30-50% and 50-70% by better combustion and increased fuel-air ratio. Imtenan et al [13] investigated on Jatropha biodiesel (JB20) blend and its altered blend with different percentage of n-butanol and diethyl ether by comparing the combustion, performance and emission characteristics. In-cylinder pressure was higher due to higher Cetane number present in JB20 in comparison to base diesel. The pressure was the consequence of retarded start of the combustion and since there was an addition of oxygenated compounds n-butanol and diethyl ether (DEE) in the blends, there was a reduction in higher latent heat of evaporation. BSFC was 5.4% higher in comparison to diesel since JB20 had very low calorific value. There was a drastic reduction in smoke opacity by around 27% and 38.5% for the blends 10% of n-butanol and 10% of DEE blend respectively.

Ong et al [14] experimented with non-edible oils like jatrophacurcas (JCB10), ceibapentandra (CPB10) and calophylluminophyllum (CIB10). Better engine performance was produced by 10% of blends along with the reduction in the exhaust emissions, except NO_x. There was a decline in BSFC for the blends of JCB10, CPB10, and CIB10. El Boulifi et al [15] performed two-step crystallization with four short-chain alcohols to get the transesterified jojoba oil. Awad [16] investigated jojoba ethyl ester by blending it with ethanol. With increase in the proportion of ethanol in the mixture, there was a decrease in the low caloric value and the fuel density decreased slightly. Al-Hamamre et al [17] studied the parameters such as dynamic viscosity, density, flash point and heating value of jojoba oil-petroleum diesel, jojoba oil-biodiesel and petroleum diesel-biodiesel blends. All the results were co-related by the polynomials obtained through regression analysis and the compatibility with other reported model were also investigated. Selim [18] reported that burning of jojoba methyl ester (JME) fuel reduced its viscosity. Adding diethyl ether (low viscosity oil) to JME led to increased reduction in the viscosity of the fuel. Heat addition to the JME did not change the exhaust gas temperature. Ignition delay period was reduced by addition of heat to JME. High pressure rise rate and combustion pressure slightly increased due to addition of DEE to JME. There was a reduction in the mechanical efficiency and an inclination in the indicated mean effective pressure due to the above reasons.

Shaafi et al [19] told that in order to decrease the peak temperature and emission (NOx), emulsification of diesel had to be done. At the same time, increase in the percentage of water in the emulsion decreased the performance characteristics as it imbibed large quantity of heat for the evaporation. The NO_x emission can be reduced with the help of nano-additives because it has the capability to accomplish equal level of micro explosion with minimal quantity of water in the emulsion because of its layer surface area contact which helped in improvisation of the performance. The present experimental investigation focuses on understanding the effect of multi walled carbon nano tubes (MWCNT) on oxygenated blends of Jojoba biodiesel. Design of experiments (DOE) technique is used to identify the stable fuel blend to be used in the CI engine. Fuel characterization is also carried out to understand the fatty acid methyl esters using GCMS and FTIR studies. The combustion, performance and emission analysis of various blends namely, D70JJBD20, D70JJBD20O10, D70JJBD20O10CNT50, D70JJBD20O10CNT100 and D70JJBD20O10CNT150 is compared with neat diesel.

2. Materials and methods

2.1. Transesterification process

Generally, raw jojoba oil is rich in viscosity. Therefore, in order to convert the heavier molecules into lighter molecules, transesterification process is performed. In this process, sodium hydroxide acts as a catalyst. The sodium methoxide is synthesized by dissolving 6.5g of NaOH in 200 ml of methanol in a distinct container and it is agitated for 30 minutes. The resultant methoxide solution is mixed with one litre of jojoba oil and the mixture is heated at 60°C aided with stirring for 60 minutes at 500 rpm speed limit. The reaction mixture is allowed to settle down on observing the process of phase

separation and cooled to room temperature. The top phase and bottom phase contains biodiesel and glycerine, a by-product which is separated by decantation. The top phase might contain excess amount of methanol soap formation and partially reacted glycerides. After the phase separation, biodiesel is cleansed by distilling the residual at 60°C. The rest of the catalyst is washed with non-ionized (distilled water) at pH 4.5 by adding 1-2 droplets of acetic acid. Anhydrous Na2So4 is then added to remove water followed by refining [20-22].

2.2. Fourier Transform Infrared (FT-IR) Spectrometer

Jojoba biodiesel (JJBD) is characterized in Spectrum one FT-IR spectrometer with a scan range MIR 450-4000 cm^{-1}, resolution 1.0 cm^{-1} to find the functional group presents in it. By the vibrational motion of the molecules present in the sample, infrared spectrum is initiated. It is used to find the depiction of organic, inorganic and biological compounds present. The change of interferogram into spectrum through mathematical formulation is done by the computer which is connected with the equipment.

2.3. Gas chromatography mass spectrometry

In order to find the saturated and unsaturated ester content present in the JJBD, JEOL GCMATE 2 is used. This GC-MS with data system is a high resolution double focusing instrument. The maximum resolution of this equipment is 6000 and maximum calibrated mass is 1500 Daltons. When it comes to application part, molar mass and structural analysis of small biomolecules, structural clarification of organic compounds are carried out under mechanistic study of fragmentation process under mass spectrometric condition.

2.4. Physiochemical properties

The detailed physiochemical properties of the raw and Trans esterified jojoba oil are compared with neat diesel as shown in Table 1. It can be noticed that the kinematic viscosity of JJBD is brought down drastically from 24.05 cSt to 3.99 cSt through trans esterification process. A minimal variation is observed in the density of raw and processed bio-oil. The flash point is also reduced significantly by up to 48°C making the JJBD more suitable as engine fuel.

Table 1: Physio-chemical properties of neat diesel, raw jojoba oil and JJBD

Property	Kinematic viscosity, cSt	Flash point, °C	Gross calorific value, kJ/kg	Density kg/m^3
Neat Diesel	2.84	68	42700	840
Raw Jojoba oil	24.05	275 - 295	31010	863.32
JJBD	3.99	48	42763	866

The property of MWCNT is illustrated in Table 2 on description of its colour, surface area, purity and its physical parameters. The variation in physiochemical properties when the oxygenated JJBD is blended with MWCNT in various proportions is tabulated in Table 3. Addition of MWCNT with the oxygenated biodiesel increased the kinematic viscosity and gross calorific value significantly. This is due to micro explosion of MWCNT at elevated temperature releasing enormous amount of energy. The kinematic viscosity and density showed a noticeable increase in its value with the increase in concentration of MWCNT [17, 23].

Table 2: Properties of MWCNT

Carbon nanotube	Description
Type	Multiwall carbon nanotube
Colour	Black powder
Surface area	370 m^2/g
Average length	1-5µm
Average diameter	10-15 nm

Table 3: Comparison of test fuel properties

Property	Kinematic. viscosity at 40°C, mm^2/s	Flash point, °C	Gross calorific value, kJ/kg	Density kg/m^3
D70 JJBD20	3.99	298	42764	867
D70 JJBD20 O10	4.01	304	44121	869
D70JJBD20 O10 CNT50	4.36	286	45470	871
D70JJBD20 O10 CNT100	4.68	282	46044	873
D70JJBD20 O10 CNT150	5.02	279	46658	875

2.5. Fuel formulation

In order to get an optimized result, Taguchi's DOE is chosen. This method is based on the orthogonal array concept which gives much reduced variance for the number of experiments to be conducted to get an optimum solution. Orthogonal array provides a set of well balanced (minimum) experiments to find a considerable optimized solution. The compositions of fuels tested are diesel, jojoba oil (transesterified), n-butanol (oxygenate) and MWCNT. The blends are prepared with the help of a magnetic stirrer in which the stirring period is kept for 30 minutes at 350-400 rpm. In order to obtain a stable blend and no agglomeration in the sample, ultra-sonication is practiced. Thus, all the samples are prepared with the help of ultra-sonication and the following fuel formulations namely, D70JJBD20O10, D70JJBD20O10CNT50, D70JJBD20 O10CNT100, and D70JJBD20O10CNT150 are obtained. Table 4 shows the orthogonal array based on the Taguchi approach. "Experiment No.8" is found to be favourable as this blend is stable and free from agglomeration.

Table 4: Test fuels based on Tauguchi's approach

Expt. No	Diesel (%)	JJBD (%)	*n*-butanol (%)	MWCNT (in ppm)
1	90(1)	10(1)	10(1)	50(1)
2	90(1)	20(2)	20(2)	100(2)
3	90(1)	30(3)	30(3)	150(3)
4	80(2)	10(1)	20(2)	150(3)
5	80(2)	20(2)	30(3)	50(1)
6	80(2)	30(3)	10(1)	100(2)
7	70(3)	10(1)	30(3)	100(2)
8	70(3)	20(2)	10(1)	150(3)
9	70(3)	30(3)	20(2)	50(1)

3. Experimentation

The Kirloskar make diesel engine is used in this present study to analyze the performance, combustion and emission of the CI engine. The specification details of

the test engine and instrumentation details are tabulated in Table 5. An eddy current dynamometer (water cooled) is connected to load the engine. The dynamometer runs at a speed varying from 1500-6000 rpm. The piezo powering unit (model AX-409) is used to find the pressure within the engine cylinder and the rotation of the flywheel i.e. crank angle. The entire data collected is routed through a data acquisition system and it is analysed using Engine Soft, engine performance analysis software. The schematic arrangement of the experimental setup is shown in Fig. 1.

Table 5: Details of test engine with instrumentation

Parameter	Description or value
Engine	Kirloskar, model TV1, single cylinder, 4 stroke diesel, water cooled, power 5.2 kW at 1500rpm, stroke 110 mm, bore 87.5 mm, 661cc, CR17.5
Dynamometer	Eddy current, water cooled
Temperature sensor	Type RTD, PT100 and, Type K thermocouple
Air box	M S fabricated with orifice meter and manometer
Piezo sensor	Range 5000 psi, with low noise cable
Data acquisition device	NI USB-6210, 16-bit, 250 kS/s
Crank angle sensor	Resolution 1 Deg, speed 5500RPM with TDC pulse
Load indicator	Digital, range 0-50 kg, supply 230 V AC
Load sensor	Load cell, type strain gauge, range 0-50 kg
Fuel flow transmitter	DP transmitter, range 0-500 mm WC
Air flow transmitter	Pressure transmitter, range (-) 250 mm WC
Rotameter	Engine cooling 40-400 LPH; Calorimeter 25-250 LPH
Overall dimensions	W2000 * D 2500 * H 1500mm

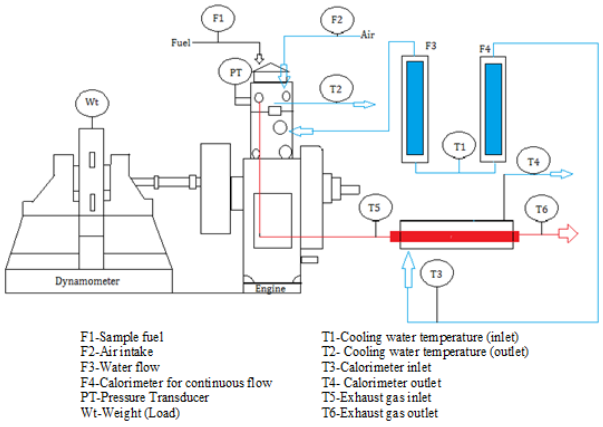

Fig. 1: Test engine schematic view

4. Results and discussion

4.1. Characterization of JJBD

The FT-IR spectrometer is used to analyse the functional groups present in the trans-esterified jojoba oil. As the infrared light is interacting with the molecules present in the sample, vibration occurs. Thus, with the help of these vibrations, the functional groups present in the oil are estimated. The concentration of each functional group is estimated with the help of band intensity of a particular compound. By interpreting the results, it is found that amine (3416 cm^{-1} band), alkene (3071 cm^{-1} band), aldehyde (2727 cm^{-1} band), aromatic (1581 cm^{-1} band), alkyl halide (1372 cm^{-1} band), acid (1278 cm^{-1} band), ether (1256 cm^{-1} band) and alcohol (1130 cm^{-1} band) compounds are present in the tested samples. Fig. 2 shows the FT-IR spectrogram of the JJBD.

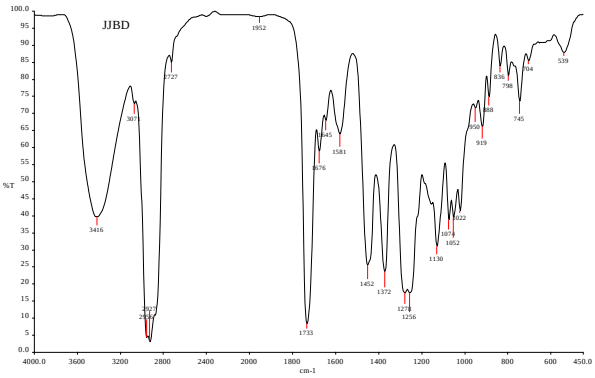

Fig. 2: FT-IR spectrogram of JJBD

GC-MS is carried out to identify the methyl ester compounds present in the trans-esterified jojoba oil in order to justify that the biodiesel is ready to be used in diesel engine. As the solution is interposed into the sample port, the solution is vaporized (separated) and carried along by an inert gas namely nitrogen or helium. The separated compounds enter into the detector which generates signals with respect to the concentration of each ester compounds present in it. On interpreting the samples, it is identified that "1, 7, 7-trimethyl-bicyclo [2.2.1] hept-2yl ester {C12H20O2}, hexadecanoic acid methyl ester {C16H32O}, 8-nonenoic acid 9-(1, 3, 6-nonatrienyloxy) - methyl ester {C18H28O3}, hepta-decanic acid methyl ester {C17H34O}, docosanoic acid methyl ester {C23H46O2} are present in the tested fuels [24-27]. This confirms that the JJBD can be used as fuel for CI engine. Fig. 3 shows the GC MS chromatogram for the JJBD sample.

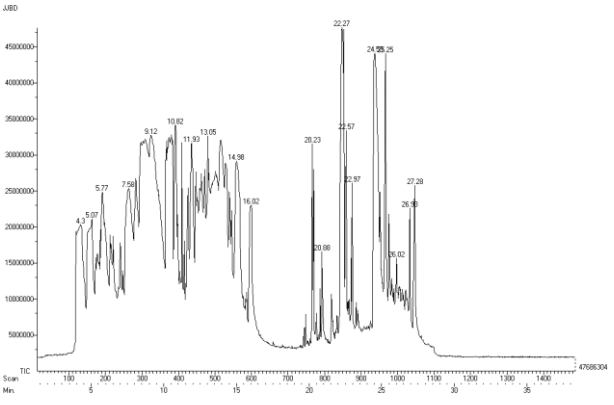

Fig. 3: GC MS chromatogram of JJBD

4.2. Engine performance characteristics

Fig. 4 shows the plot between BTE and brake mean effective pressure (BMEP). On comparing the BTE parameter of diesel with tested fuel blends, most of the tested fuel blends showed lower values. This is due to better optimal viscosity of the base fuel (diesel) and the perceived easily chargeable (i.e., volatile in nature) fuel.

Among all the fuel blends, the composition D70JJBD20O10CNT100 shows a better efficiency curve. Even though n-butanol is used as oxygenated additives in four samples, only D70JJBD20O10CNT100 gives an optimized result. The lowest BTE curve is obtained for the compositions of D70JJBD20O10 and D70JJBD20O10CNT50. This is due to its lower air-fuel mixture and worst volatility (fuel) in nature. Therefore, it might have taken more time for the ignition to occur in the combustion chamber which led to increase in ignition delay parameter. The speed of the engine is 1500 rpm and the BTE for D70JJBD20 blend shows 0.47 %, 20.02 %, 29.88 %, 31.32 %, and 33.32 % with respect to the different load applied as seen in Fig. 4. On the other hand, D70JJBD20O10CNT150 fuel blend gives the BTE of 0.19 %, 20.08 %, 28.47 %, 32.86 %, and 32.95 % from lowest to highest loading conditions. As the content of the nanoparticle is being increased in the fuel samples, complete combustion takes place due to better air-fuel mixture ratio in the nano fuel samples [26, 28].

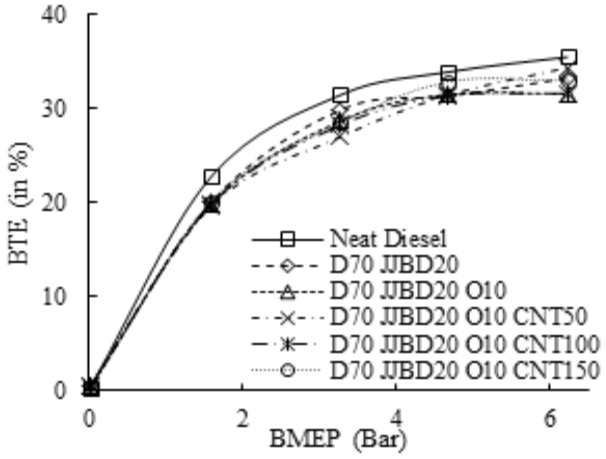

Fig. 4: Variations in BTE with BMEP

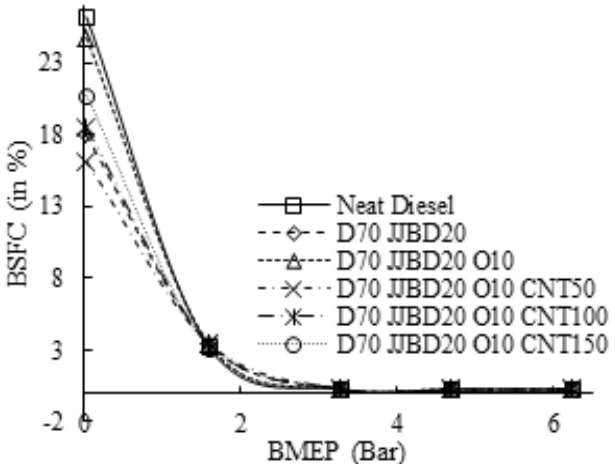

Fig. 5: Variations in BSFC with BMEP

Fig. 5 shows the variations of BSFC with brake mean effective pressure. On comparing with the neat diesel, the other fuel blends shows a declension in the BSFC. The fuel samples such as D70JJBD20, D70JJBD20O10, D70JJBD20O10CNT50, D70JJBD20O10CNT100 and D70JJBD20O10CNT150 shows a BSFC value of 0.25%, 0.27%, 0.25%, 0.27% and 0.26 % respectively for full loading condition. While at partial loading conditions, these samples show a value of 0.28%, 0.28%, 0.29%, 0.31% and 0.30% respectively. It is observed that the fuel blends which contains MWCNT, the value of BSFC parameter decreases in a gradual manner [29, 30].

4.3. Engine combustion characteristics

The comparison of in-cylinder pressure with respect to crank angle is represented in Fig. 6. Generally, an increase in viscosity of the fuel leads to an ignition delay which affects the evaporation and atomization of fuel leading to improper combustion in the cylinder. The results showed that the increase in the percentage of loading conditions leads to an increase in the peak pressure within the combustion chamber thereby leading to a vigorous combustion to take place with respect to particular crank angle. While comparing all the compositions for no load conditions, D70JJBD20 shows the highest peak pressure (45.135 bar) which asserts that maximum combustion takes place in it at no load conditions. But, at partial loading conditions, the composition D70JJBD20O10 shows 59.327 bar for the crank angle at 369°. At no load conditions, the compositions D70JJBD20, D70JJBD20O10, D70JJBD20O10 CNT50, D70JJBD20O10CNT100 and D70JJBD20O10CNT150 show 45.135 bar (at 369° crank angle), 43.8095 bar (at 369° crank angle), 42.336 bar (at 373° crank angle), 41.973 bar (at 374º crank angle) and 42.162 bar (at 374° crank angle) respectively. When the engine is tested at partial loading conditions, the fuel blends namely D70JJBD20, D70JJBD20O10, D70JJBD20O10 CNT50, D70JJBD20O10CNT100 and D70JJBD20O10CNT150 shows an in-cylinder pressure of around 58.370 bar (at 370° crank angle), 59.327 bar (at 369° crank angle), 59.094 bar (at 369° crank angle), 58.065 bar (at 369° crank angle) and 58.139 bar (at 371° crank angle) respectively. At full load conditions, the composition of D70JJBD20O10 shows in-cylinder pressure of 67.312 bars for crank angle at 370°. The compositions D70JJBD20O10CNT50, D70JJBD20O10CNT100 and D70 JJBD20O10CNT150 show a maximum in-cylinder pressure of 42.337 bar, 41.9734 bar and 42.162 bar respectively [31].

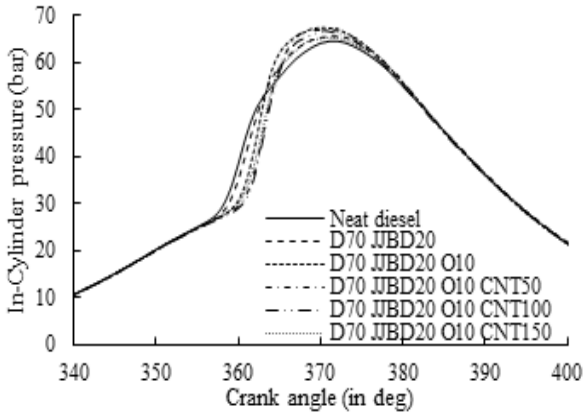

Fig. 6: Variation of in-cylinder pressure at full load condition

The variation of rate of heat release (ROHR) with crank angle is shown in Fig. 7. Generally, ignition delay is caused due to poor atomization and evaporation of the fuel as it enters the combustion chamber. As can be seen in Fig. 7, instantaneous ignition is observed within the

combustion chamber. At no load conditions, the fuel compositions D70JJBD20, D70JJBD20O10, D70JJBD20O10CNT50, D70 JJBD20O10CNT100 and D70JJBD20O10CNT150 shows a ROHR of 41.445 J/CAD (at 364° crank angle), 41.295 J/CAD (at 366° crank angle), 37.432 J/CAD (at 367° crank angle), 39.518 J/CAD (at 368º crank angle) and 38.419 J/CAD (at 368° crank angle) respectively. As the loading capacity is increased to 50% loading conditions, all the compositions namely, D70JJBD20O10CNT50, D70JJBD20O10CNT100 and D70JJBD20O10CNT150 show an increase in the rate of heat release to 89.703 J/CAD (at 365° crank angle), 84.078 J/CAD (at 365° crank angle) and 80.633 J/CAD (at 364° crank angle) respectively. This shows that the addition of MWCNT in appropriate proportions to the fuel blends increase the thermal conductivity, thereby enhancing the instant ignition of fuel droplets. On comparing with the reference fuel (diesel), a higher rate of heat release is observed in the all the fuel samples. At full load conditions, the compositions D70JJBD20, D70JJBD20O10, D70JJBD20O10CNT50, D70JJBD20O 10CNT100 and D70JJBD20 O10CNT150 show ROHR of 64.185 J/CAD (at 361° crank angle), 90.0839 J/CAD (at 363° crank angle), 89.924 J/CAD (at 363° crank angle), 89.886 J/CAD (at 363° crank angle), 85.4204 J/CAD (at 363° crank angle) and J85.420 J/CAD (at 363° crank angle).

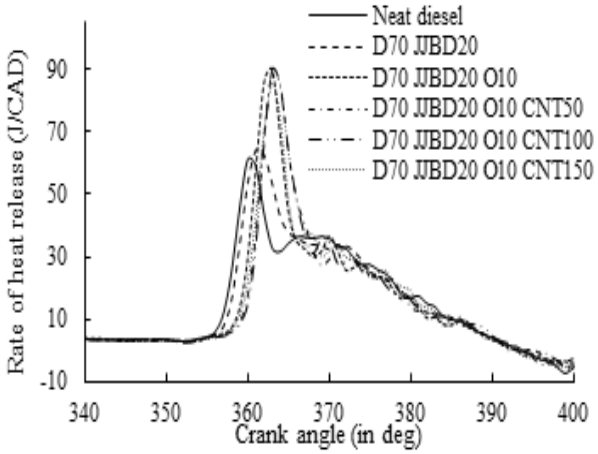

Fig. 7: Variation in rate of heat release at full load condition

The relationship between cumulative heat release rates (CHRR) with respect to crank angle is shown in Fig. 8. An increase in temperature of the cylinder wall chamber enhances the atomization and evaporation of the fuel. As the percentage of the loading condition is increased, simultaneously there is an augmentation of cumulative heat release rate in every tested fuel. At no-load conditions, the compositions D70JJBD20, D70JJBD20O10, D70JJBD20O10CNT50, D70JJBD20O10 CNT100 and D70JJBD20O10CNT150 show CHRR of 0.5224 kJ (at 387° crank angle), 0.5099 kJ (at 387° crank angle), 0.4604 kJ(at 386° crank angle), 0.4948 kJ(at 387° crank angle) and 0.4993 kJ (at 387°crank angle) respectively. The compositions D70JJBD20 and D70JJBD20O10 give the highest cumulative heat release rate at around 1.007 kJ (at 393º crank angle) and 1.0058 kJ (at 393° crank angle) when compared with other test fuels at full-load conditions. At full load conditions, the fuel samples D70 JJBD20, D70JJBD20O10, D70JJBD20O10CNT50, D70JJBD20O10CNT100 and D70JJBD20O10 CNT150 indicates a value of 1.0012 kJ (at 393° crank angle), 1.007 kJ (at 393° crank angle), 0.9976 kJ (at 393° crank angle), 1.0058 kJ (at 393° crank angle), 0.9976 kJ (at 392° crank angle) and 0.9938 kJ (at 392° crank angle) respectively.

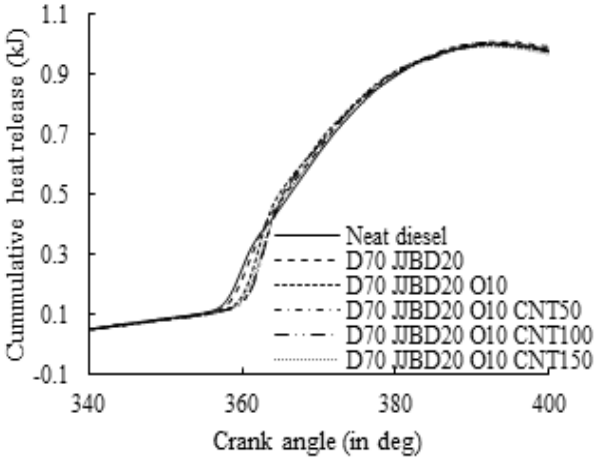

Fig. 8: Variation in cumulative heat release rate at full load condition

The variation of rate of pressure rise (ROPR) with crank angle is shown in Fig. 9. As the fuel enters the combustion chamber which is at high temperature, secondary atomization and micro-explosion of fuel occurs. Therefore, an instantaneous combustion occurs which leads to rapid rise in the pressure. A fast combustion along with initiation of ignition lead to an increase in peak pressure and pressure rise rate. The fuel compositions D70JJBD20, D70JJBD20O10, D70JJBD20O10 CNT50, D70JJBD20O10CNT100 and D70JJBD20O10CNT150 at no load condition shows a ROPR of 2.581 bar (at 365° crank angle), 3.41 bar (at 364° crank angle), 2.998 bar (at 366° crank angle), 2.441 bar (at 366° crank angle) and 2.391 bar (at 367° crank angle) respectively. At full-load conditions, these composition shows a ROPR of 6.2788 bar (at 361° crank angle), 8.2954 bar (at 362° crank angle), 8.4113 bar (at 363° crank angle), 8.4229 bar (at 363° crank angle), and 7.912 bar (at 363° crank angle). On comparing all the fuel blends, the MWCNT blended fuel namely D70 JJBD20O10CNT50 and D70JJBD20O10CNT100 gives the higher rate of pressure rise.

The relationship between the ignition delay and BMEP is shown in Fig. 10. On comparing all the tested fuel blends with neat diesel, there is a reduction in the ignition delay which asserts that instant ignition takes place within the combustion chamber as early as possible. There are two types of ignition delay namely physical delay (which include the atomization of fuel and vaporization) and chemical delay (pre-mix combustion phase, Cetane number). Generally, higher Cetane number of the fuel leads to reduction in the occurrence period of ignition delay. The Cetane number of n-butanol and transesterified jojoba oil is 25 and 63.5. The ignition delay for D70JJBD20, D70JJBD20O10,

D70JJBD20O10CNT50, D70JJBD20 O10CNT100 and D70JJBD20O10CNT150 at no-load conditions is 8.47°, 8.15°, 7.98°, 7.87° and 7.66° respectively. As the load increases, there is a declination in the time taken for the ignition to occur in the combustion chamber. These compositions at full load conditions show an ignition delay of 3.14°, 3.01°, 2.87°, 2.61° and 2.57°.

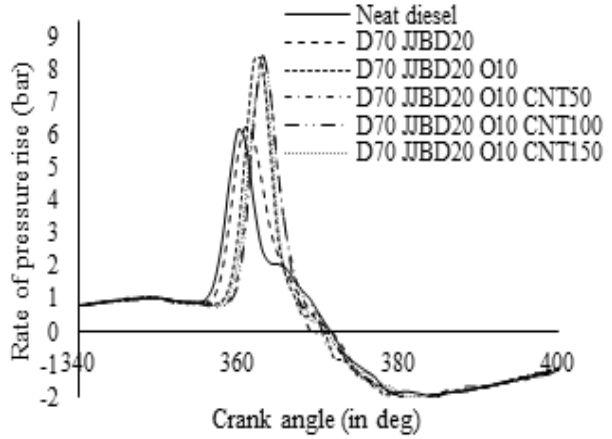

Fig. 9: Variation in rate of pressure rise at full load condition

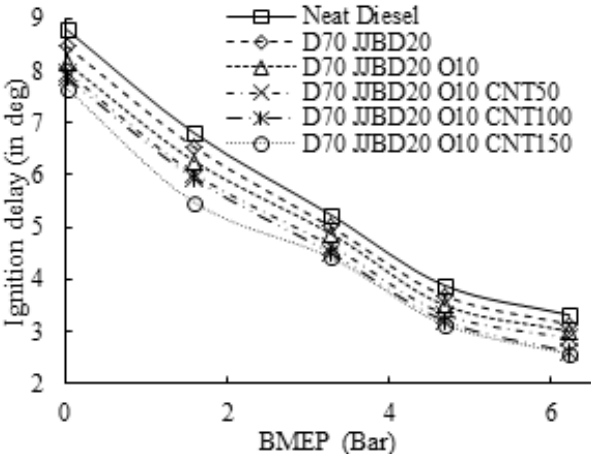

Fig. 10: Variation in ignition delay with BMEP

4.4. Engine emission characteristics

Fig. 11 shows the variations in unburnt hydrocarbon (UBHC) emissions with respect to BMEP. On comparing with the base diesel, the composition D70JJBD20O10 gives the unburnt hydrocarbon emissions similar to diesel. The footprint of UBHC for the composition D70JJBD20 O10 is 23 ppm, 25 ppm, 28 ppm, 36 ppm and 54 ppm from no load to full load conditions. Adding n-butanol, an oxygenated agent, to the fuel blends with MWCNT enhances the combustion. At full load, the UBHC emission for D70JJBD20O10CNT50, D70JJBD20O10CNT100 and D70JJBD20O10 CNT150 is 56 ppm, 52 ppm and 49 ppm. At no load condition, the composition D70JJBD20 shows 12 ppm of UBHC emission. Subsequently at 25%, 50%, 75% and 100% loading conditions, the UBHC emissions is around 16 ppm, 21 ppm, 27 ppm and 46 ppm respectively. Depending on the nature of nano particle used, a healthy combustion takes place in the combustion chamber and the emissions of UBHC may increase or decrease. Moreover, it also depends on the viscosity of the fuel as it influences the capacity of the fuel to vaporize and time leading to ignition delay. As can be seen in Fig. 11, the composition D70JJBD20O10CNT50 shows a higher UBHC emission of 33 ppm, 35 ppm, 36 ppm, 41 ppm and 53 ppm for the load varying from no load to full load conditions [32].

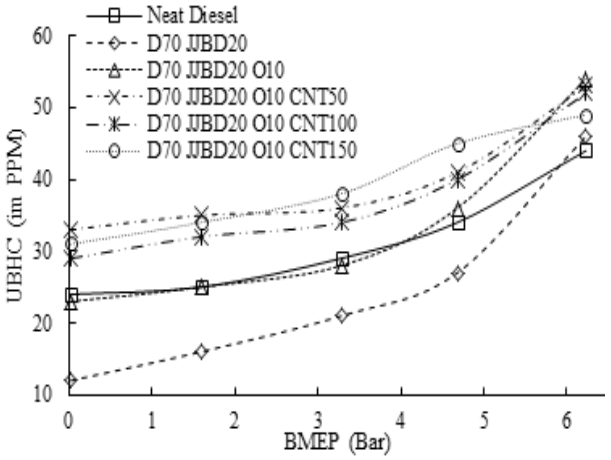

Fig. 11: Variation in UBHC emission with BMEP

Fig. 12 shows the variations in carbon mono oxide (CO) emission with BMEP. As can be observed in Fig. 12, a large amount of CO is exhausted from the engine for all test fuels except diesel. There is a gradual decrease in CO emissions till 50% loading conditions (3.28 bar) excluding diesel as other test fuels has enough oxygen content due to addition of n-butanol. However, after 50% load conditions, there is a sudden increase in the CO emissions. At higher loads, D70JJBD20 O10CNT100 composition shows CO emission of 0.332% whereas neat diesel exhausts only 0.112%. At no load condition, the compositions D70JJBD20O10 and D70JJBD20O10CNT150 shows 0.079% CO emission while diesel shows 0.049% of CO emission from the exhaust. On comparing all the blends, D70JJBD20O10CNT150 composition shows an optimized CO emission with MWCNT addition.

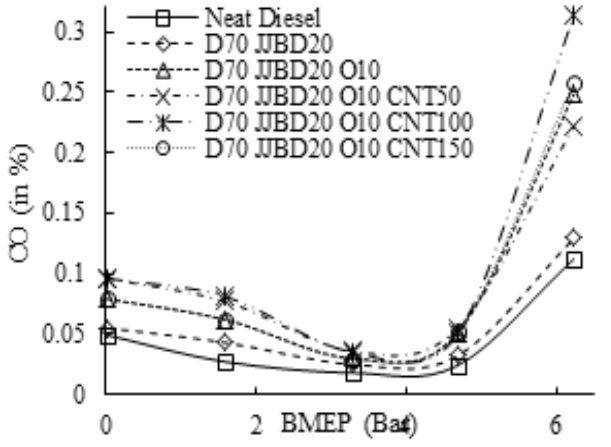

Fig. 12: Variation in CO emission with BMEP

In general, carbon mono oxide gets emitted because of incomplete combustion occurring in the combustion chamber. However, the addition of MWCNT has its unique contribution to these blends. The CO emission occurs at a higher rate when compared with neat diesel

CO emission. As the proportion of this MWCNT is increased, CO emission also increases. While the composition D70JJBD20O10CNT100 shows an emission of 0.096%, 0.081%, 0.035%, 0.05% and 0.313% for load varying from no load to full load, the composition D70JJBD20O10CNT150 show a reduced CO emission of 0.079%, 0.062%, 0.029%, 0.052% and 0.0258% for the same loading conditions. Moreover, the fuel sample without MWCNT i.e., D70 JJBD20 shows a reduced CO emission compared to other blended fuels.

Fig. 13 shows the variation in CO_2 emissions with BMEP. As can be seen in the Figure, the blended fuels show a more or less similar trend. At no load and 75% of the load conditions, base diesel and D70JJBD20O10CNT150 shows an equal amount of CO_2 emissions (1.87% and 6.89%). D70JJBD20O10CNT100 shows a slightly better reduced CO_2 emission at all loading conditions and this composition can be considered as an optimized one. Moreover, D70JJBD20 shows the highest CO_2 emission (2.11%, 3.59%, 5.32%, 6.97%, and 9.17%) at all loading conditions when compared with other blends. This establishes the fact that an increase in the wall temperature of the combustion chamber results in complete combustion to take place for this composition of fuel. The second highest CO_2 emission is given by D70JJBD20O10. Eventually, as the MWCNT is added in proportions to the fuel, there is an augmentation in combustion process. This could be correlated with CO_2 emission. Thus, the presence of MWCNT increases the combustion characteristics of the fuel in an indirect manner.

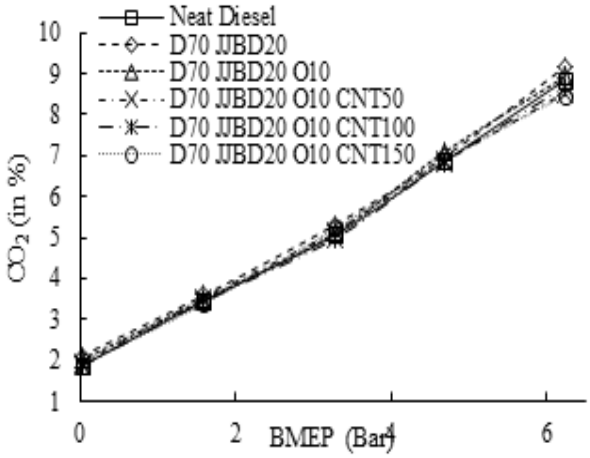

Fig. 13: Variation in CO_2 emission with BMEP

Fig. 14 shows the variations in NOx emission with BMEP. Even though the fuel samples are blended with an oxygenate (n-butanol), the addition of MWCNT to it dominates the fuel blends by emitting large amount of nitric oxide (NO) and nitrogen dioxide (NO_2) which combines to form oxides of nitrogen (NO_x). Higher the concentration of oxygen in the blends, then the combustion takes place in a heterogeneous manner. The NOx formation is also influenced by the dimension of the engine and ignition delay period. The above Figure depicts the NOx footprint exhausted from the CI engine through an exhaust outlet. The composition D70JJBD20O10CNT150 shows the highest NOx emissions at no load and full load conditions as 183 ppm and 1652 ppm respectively. This establishes that a vigorous combustion has taken place in the combustion chamber. This could be correlated with the ROPR which is discussed earlier. However, D70JJBD20O10CNT100 shows a lesser NOx emission when compared with other blended fuels at all load conditions. D70 JJBD20O10CNT100 composition emits NOx of 166 ppm, 487 ppm, 1081 ppm, 1574 ppm and 1690 ppm from no load to full conditions. This MWCNT blend is found to be an optimum one.

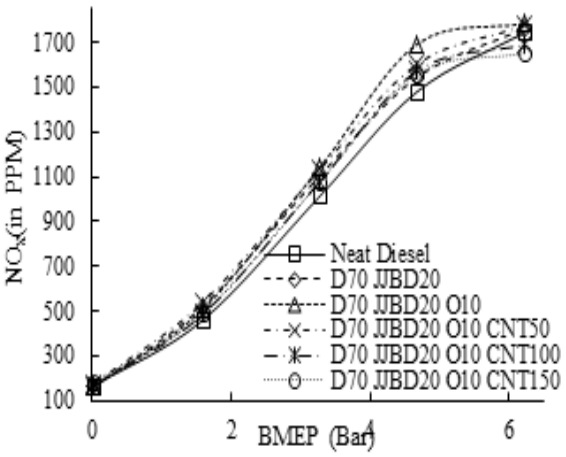

Fig. 14: Variation in NO_x emission with BMEP

Fig. 15 shows the variations in smoke emissions with BMEP. Generally, smoke emission is regarded as visible emission as this parameter indicates that the combustion which took place in the combustion chamber is complete or an incomplete combustion. The smoke emission readings are measured with the help of "Light Extinction type" where in a light source is kept at the opposite passage of the incoming smoke. Thus, the smoke blocks the light source such that the intensity of the light source reduces and the smoke opacity is estimated.

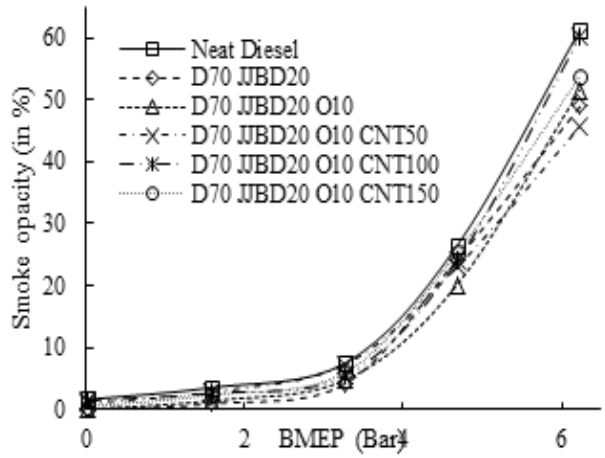

Fig. 15: Variation in smoke emission with BMEP

D70JJBD20 composition shows the least smoke exhaust (viz., 0%, 0.9%, 4.2%, 24.2% and 48.9% for the respective load conditions) from the engine. Among all MWCNT fuel blends, the smoke opacity of D70JJBD20O10CNT50 composition is the least (i.e., 1%, 2.8%, 7.3%, 23% and 45.7%) at all load conditions. At 75% load condition, there is a reduction of 4.16% in

smoke opacity for the composition D70JJBD20O10 CNT150 with neat diesel. The MWCNT composition D70JJBD20O10CNT100 shows the highest smoke opacity at all loads by 1.4%, 2.6%, 5.5%, 23.9%, and 60.2%.

5. Conclusions

Based on the experimental investigations using MWCNT in jojoba biodiesel-diesel blends along with n-butanol, the following points are drawn:

- Use of oxygenated additives (n-butanol and MWCNT) for the combustion process reduced the brake thermal efficiency and increased the fuel economy.
- At full load condition, the composition D70JJBD20O10CNT100 shows a 12.5% increase in the BSFC parameter compared to base diesel.
- The composition D70JJBD20O10CNT150 shows a reduction of 0.744% of cumulative heat release at full load condition.
- The in-cylinder pressure and the rate of pressure rise are improved in MWCNT blends along with reduction ignition delay period.
- Rate of pressure rise for the blend D70JJBD20O10CNT100 at full load condition is increased by 36.35% compared to diesel.
- A considerable reduction in smoke opacity is observed in the MWCNT blends due to enhanced oxygen content in the fuel. The smoke opacity is reduced by 4.34% for the composition of D70JJBD20O10CNT100.
- An increase in 5.34% of oxides of nitrogen is observed for the composition D70JJBD20O10 CNT100 at full load condition on comparison with diesel.
- Vigorous burning or increase in rate of combustion is observed due to the addition of oxygenated additives.
- Due to the better combustion process, the carbon dioxide emissions by MWCNT blends is lesser compared to diesel.

Based on this study, it can be concluded that D70JJBD20O10CNT100 blend is the optimum which gives a better combustion and performance characteristics along with reduced emissions.

REFERENCES:

[1] R.P.S. Chakradhar and V.D. Kumar. 2012. Water-repellent coatings prepared by modification of ZnO nanoparticles, *Spectrochimica Acta Part A*, 94, 352-356. https://doi.org/10.1016/j.saa.2012.03.079.

[2] M. Canakci, A.N. Ozsezen and A. Turkcan. 2009. Combustion analysis of preheated crude sunflower oil in IDI diesel engine, *Biomass and Bioenergy*, 33, 760-767. https://doi.org/10.1016/j.biombioe.2008.11.003

[3] L. Siwale, L. Kristof, T. Adam, A. Bereczky, M. Mbarawa, A. Penninger and A. Kolesnikov. 2013. Combustion and emission characteristics of n-butanol/diesel fuel blend in a turbo-charged compression ignition engine, *Fuel*, 107, 409-418. https://doi.org /10.1016/j.fuel.2012.11.083.

[4] B. Tesfa, R. Mishra, C. Zhang, F. Gu and A.D. Ball. 2013. Combustion and performance characteristics of CI (compression ignition) engine running with biodiesel, *Energy*, 51, 101-115. https://doi.org/10.1016/j.energy .2013.01.010.

[5] K. Anand, R.P. Sharma and P.S. Mehta. 2011. Experimental investigation on combustion, performance and emission characteristics of neat karanja biodiesel and its methanol blend in a diesel engine, *Biomass and Bioenergy*, 35, 533-541. https://doi.org/10.1016/j. biombioe.2010.10.005.

[6] R.K. Maurya. 2011. Experimental study of combustion and emission characteristics of ethanol fuelled port injected homogeneous charge compression ignition (HCCI) combustion engine, *Applied Energy*, 88, 1169-1180. https://doi.org/10.1016/j.apenergy.2010.09.015.

[7] A.I.E. Seesy, A.K.A. Rahman, M. Bady and S. Ookawara. 2017. Performance, combustion and emission characteristics of a diesel engine fuelled by biodiesel-diesel mixtures with multi-walled carbon nanotubes additives, *Energy Conversion & Management*, 135, 373-393. https://doi.org/10.1016/j.enconman.2016.12.090.

[8] V. Saxena, N. Kumar, V.K. Saxena. 2017. A comprehensive review on combustion and stability aspects of metal nanoparticles and its additive effect on diesel and biodiesel fuelled C.I. engine, *Renewable and Sustainable Energy Reviews*, 70, 563-588. https://doi.org/10.1016/j.rser.2016.11.067.

[9] M. Annamalai, B. Dhinesh, K. Nanthagopal, P.S. Krishnan, J.I.J.R. Lalvani, M. Parthasarathy and K. Annamalai. 2016. An assessment on performance, combustion and emission behaviour of a diesel engine powered by ceria nanoparticle blended emulsified biofuel, *Energy Conversion and Management*, 123, 372-380. https://doi.org/10.1016/j.enconman.2016.06.062

[10] H.A. Choudhury, R.S. Malani, S. Vijayanand and Moholkar. 2013. Acid catalyzed biodiesel synthesis from jatropha oil: Mechanistic aspects of ultrasonic intensification, *Chemical Engg., J.*, 231, 141-150. https://doi.org/10.1016/j.cej.2013.06.107.

[11] G. Paul, A. Datta and B.K. Mandal. 2014. An experimental and numerical investigation of the performance, combustion and emission characteristics of diesel engine fueled with jatropha biodiesel, *Energy Proc.*, 54, 455-467. https://doi.org/10.1016/j.egypro .2014.07.288.

[12] H. Raheman and S. Kumari. 2014. Combustion characteristics and emissions of a compression ignition engine using emulsified jatropha biodiesel blend, *Biosystems Engg.*, 123, 29-39. https://doi.org/10.1016/j .biosystemseng.2014.05.001.

[13] S. Imtenan, H.H. Masjuki, M. Varman, I.M. Rizzwanul Fattah, H. Sajjad and M.I. Arbab. 2015. Effect of n-butanol and diethyl ether as oxygenated additives on combustion-emission-performance characteristics of a multiple cylinder diesel engine fueled with diesel-jatropha biodiesel blend, *Energy Conservation and Management*, 94, 84-94. https://doi.org/10.1016/j. enconman.2015.01.047.

[14] H.C. Ong, A.S. Silitonga, H.H. Masjuki, T.M.I. Mahila and W.T. Chong. 2013. Production and comparative fuel properties of biodiesel from non-edible oils: jatrophacurcas, Sterculiafoetida and Ceibapentandra biodiesel in a CI diesel engine, *Energy Conversion and Management*, 73, 245-255. https://doi.org/10.1016/ j.enconman.2013.04.011.

[15] N.E. Boulifi. 2015. Fatty acid alkyl esters and monounsaturated alcohols production from jojoba oil using short-chain alcohols for bio refinery concepts, *Industrial Crops and Products*, 69, 244-250. https://doi.org/10.1016/j.indcrop.2015.02.031

[16] A.S. Awad. 2014. Jojoba ethyl ester production and properties of ethanol blends, *Fuel*, 124, 73-75. https://doi.org/10.1016/j.fuel.2014.01.106.

[17] A. Hamamre and A. Salaymeh. 2014. Physical properties of (jojoba oil + biodiesel), (jojoba oil + diesel) and (biodiesel + diesel) blends, *Fuel*, 123, 175-188. https://doi.org/10.1016/j.fuel.2014.01.047.

[18] M.Y.E. Selim. 2009. Reducing the viscosity of jojoba methyl ester diesel fuel and effects on diesel engine performance and roughness, *Energy Conversion and Management*, 50, 1781-1788. https://doi.org/10.1016/j.enconman.2009.03.012.

[19] T. Shaafi, K. Sairam, A. Gopinath, G. Kumaresan and R. Velraj. 2015. Effect of dispersion of various nano additives on the performance and emission characteristics of a CI engine fueled with diesel, biodiesel and blends - A review, *Renewable and Sustainable Energy Reviews*, 49, 563-573. https://doi.org/10.1016/j.rser.2015.04.086.

[20] V. Hariram, V. Pradhap, S. Seralathan, R. Jaganathan, J.G. John and M. Rajasekaran. 2018. Effect of DEE oxygenate on diesel in algal biodiesel-diesel blends on the combustion phenomenon of di compression ignition engine, *Int. J. Vehicle Structures and Systems*, 8(1), 46-53. https://doi.org/10.4273/ijvss.10.1.11.

[21] H. Venu, V. Madhavan. 2016. Effect of Al_2O_3 nanoparticles in biodiesel-diesel-ethanol blends at various injection strategies: Performance, combustion and emission characteristics, *Fuel*, 186, 176-189. https://doi.org/10.1016/j.fuel.2016.08.046.

[22] J.S. Basha and R.B. Anand. 2012. Effect of nanoparticle additive in the water-diesel emulsion fuel on the performance, emission and combustion characteristics of a diesel engine, *Alexandria Engg., J.*, 59, 164-181. https://doi.org/10.1504/IJVD.2012.048692.

[23] E.G. Varuvel, N. Mrad, M. Tazerout and F. Aloui. 2012. Experimental analysis of biofuel as an alternative fuel for diesel engines, *Applied Energy*, 94, 224-231. https://doi.org/10.1016/j.apenergy.2012.01.067.

[24] A.S.A. Awad, M.Y.E. Selim, A.F. Zeibak and R. Moussa. 2014. Jojoba ethyl ester production and properties of ethanol blends, *Fuel*, 124, 73-75. https://doz .org/10.1016/j.fuel.2014.01.106.

[25] N.E. Boulifi, M. Sanchez, M. Martinez and J. Aracil. 2015. Fatty acid alkyl esters and monounsaturated alcohols production from jojoba oil using short-chain alcohols for bio refinery concepts, *Industrial Crops and Products*, 69, 244-250. https://doi.org/10.1016/j.indcrop .2015.02.031.

[26] M.Y.E. Selim. 2009. Reducing the viscosity of jojoba methyl ester diesel fuel and effects on diesel engine performance and roughness, *Energy Conversion and Management*, 50, 1781-1788. https://doi.org/10.1016 /j.enconman.2009.03.012.

[27] M. Shah, S. Ali, M. Tariq, N. Khalid, F. Ahmad and M.A. Khan. 2014. Catalytic conversion of jojoba oil into biodiesel by organotin catalysts, spectroscopic and chromatographic characterization, *Fuel*, 118, 392-397. https://doi.org/10.1016/j.fuel.2013.11.010.

[28] V. Hariram, J.G. John and S. Seralathan. 2017. Spectrometric analysis of algal biodiesel as fuel derived through base catalyzed transesterification, *Int. J. Ambient Energy*. https://doi.org/10.1080/01430750.2017.1381153.

[29] Barabas and Touorut. 2010. Performance and emission characteristics of CI engine fueled with diesel-biodiesel, bio-ethanol blends, *Fuel*, 89, 3827-32. https://doi.org/ 10.1016/j.fuel.2010.07.011

[30] M.Y.E. Selim. 2009. Reducing the viscosity of jojoba methyl ester diesel fuel and effects on diesel engine performance and roughness, *Energy Conversion and Management*, 50, 1781-1788. https://doi.org/10.1016 /j.enconman.2009.03.012

[31] N.R. Banapurmath and R. Sankara. 2014. Experimental investigation on direct injection diesel engine fueled with graphene, silver and MWCNT- biodiesel blended fuels, *Int. J. Automot. Eng. Tech.*, 129-38.

[32] H. Venkatesan, S. Sivamani, S. Sampath, V. Gopi and M.D. Kumar. 2017. A comprehensive review on the effect of nano metallic additives on fuel properties, engine performance and emission characteristics, *Int. J. of Renewable Energy Research*, 7(2), 825-843.